Characteristics of Quantum Dash Laser under the Rate Equation Model Framework

Zahed M. Khan, Tien K. Ng and Boon S. Ooi*

Division of Physical Sciences & Engineering

King Abdullah University of Science & Technology (KAUST), Thuwal - 21534, Saudi Arabia

*email: boon.ooi@kaust.edu.sa

Abstract- **The authors present a numerical model to study the carrier dynamics of InAs/InP quantum dash (QDash) lasers. The model is based on single-state rate equations, which incorporates both, the homogeneous and the inhomogeneous broadening of lasing spectra. The numerical technique also considers the unique features of the QDash gain medium. This model has been applied successfully to analyze the laser spectra of QDash laser.**

I. INTRODUCTION

InP-based quantum dash (QDash) devices have been the area of active research from the last few years because of its superior performance characteristics, possible long wavelength tuning and applications in optical communication and networking [1]. Various theoretical approaches have been reported in literature that utilized QDashes as the active medium to examine the emission and performance characteristics of the devices. For instance, models based on computing the energy band diagram in general, applied to QDash semiconductor optical amplifiers (SOA) [2] and lasers [3] has been reported. Rate equation models based on semi-classical multimode laser field theory approach [4] has been applied to QDash lasers while the density matrix formalism [5] have been utilized to QDash SOA. In this paper, we propose to extend this density matrix formalism rate equation model [5,6] to investigate the carrier dynamics of QDash lasers. To our knowledge, such a formulation for studying QDash lasers has not been reported. The model incorporates the unique features of the QDash gain medium, the homogeneous and inhomogeneous broadening of the laser spectra. The model is applied to calculate the lasing spectra of a InAs/InP QDash laser.

I. THEORETICAL MODEL

The theoretical model is developed from the rate equations of each QDash ensemble utilizing a similar procedure reported in [6] for InAs/InP quantum dot (QD) lasers with similar assumptions, and [5] for QDash SOA. The QDashes are grouped according to their resonant wavelength and a series of longitudinal cavity photon modes are considered. Moreover, for simplicity, the difference in the resonant energies of the photon modes and the QDash ensembles are treated to be identical. The energy band diagram utilized in the simulation model is shown in Fig. 1. The model takes into account only a single ground state (GS) energy corresponding to a QDash ensemble. The reservoir of carriers, in this case, is the separate-confined heterostructure (SCH) followed by the wetting layer (WL). The associated time constants are τ_{SW} (relaxation from SCH to WL), τ_{WD} (relaxation from WL to QDash), τ_{DW} (re-excitation from QDash to WL), τ_{WS} (re-excitation from WL to SCH), and τ_S, τ_W, τ_D corresponding to
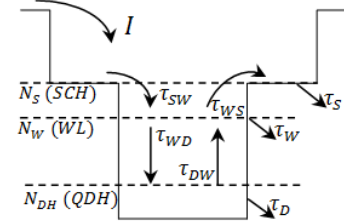

Fig. 1 Energy diagram of the QDash laser including the SCH, WL and the GS energy states with respective time constants.

the recombination in SCH, WL and QDash layers, respectively. It is noteworthy to mention that, apart from interacting with each other through the WL, the QDash groups high density of states (DOS) energy tail provides another crosstalk mechanism. The rate equation model is as follows:

$$\frac{dN_S}{dt} = \frac{I}{e} - \frac{N_S}{\tau_{SW}} - \frac{N_S}{\tau_S} + \frac{N_W}{\tau_{WS}} \tag{1}$$

$$\frac{dN_W}{dt} = \frac{N_S}{\tau_{SW}} + \sum_i \sum_k \frac{N_{j,k}}{\tau_{DW}^{j,k}} - \frac{N_W}{\tau_{WD}} - \frac{N_W}{\tau_{WS}} - \frac{N_W}{\tau_W} \tag{2}$$

$$\frac{dN_{j,k}}{dt} = \frac{N_W G_{j,k}}{\tau_{WD}^{j,k}} - \frac{N_{j,k}}{\tau_{DW}^{j,k}} - \frac{N_W}{\tau_D} - \frac{c\Gamma}{n_r} \sum_m g_m^{j,k} S_m \tag{3}$$

$$\frac{dS_m}{dt} = \sum_k \frac{N_{m,k}}{\tau_{Sp}} + \frac{c\Gamma}{n_r} \sum_k \sum_j g_m^{j,k} S_m - \frac{S_m}{\tau_p} \tag{4}$$

Eqns. (1) and (2) refer to the dynamics governing the carrier density in the SCH (N_S) and the WL (N_W) whereas Eqn. (3) corresponds to the carrier dynamics in each of the intra-dash energy levels ($N_{j,k}$) of QDash group. The subscripts j and k refers to the jth group of QDash ensemble and its kth intradash energy level. Eqn. (4) corresponds to the carrier photon density of the mth mode including the spontaneous emission term and the photon loss. The linear optical gain $g_m^{j,k}$ that refers to the kth state j^{th} QDash group contributing to the mth mode photons is given below which is based on the density matrix equation [1,2,5]:

$$g_m^{j,k} = \frac{2\pi e^2 \hbar N_D}{c n_r \epsilon_0 m_0^2} \frac{|M_{cv}|^2}{E_{cv}} (2P_{j,k} - 1) G_{j,k} B(E_m - E_{j,k}) \tag{5}$$

The details of various terms in Eqn. (5) are reported in literature [1,2,5]. In brief, $g_m^{j,k}$ incorporates both, the homogeneous, $B(E_m-E_{j,k})$ and the inhomogeneous, $G_{j,k}$, broadening. Moreover, it is worth mentioning that N_D and $G_{j,k}$ includes the unique features of the QDash by considering the quantum wire (Qwire) like density of state (DOS) function

Parameter	Description	Value	Unit
l	Cavity length	500	μm
W	Stripe width	40	μm
L_{DH}	QDash length	80	nm
W_{DH}	QDash width	20	nm
H_{DH}	QDash height	2	nm
n_l	Number of QDash layers	4	-
A_{DH}	QDash effective crossection area	1.3e-12	cm^2
C_F	Confinement factor	0.01	-
$R_1 = R_2$	Cleaved facet reflectivity	0.3	-
α_i	Internal modal loss	10	cm^{-1}
β	Spontaneous emission factor	1e-4	-
N_D	QDash density of states	4e17	cm^{-3}
D_g	QDash ground state degeneracy	1	-
D_W	WL density of states	1.8e19	cm^{-3}
E_{CV}	Central transition energy	805	meV
E_{WL}	WL ground state energy	916	meV
$\hbar\Gamma_{ih}$	Inhomogeneous broadening	12	meV
$\hbar\Gamma_g$	Homogeneous broadening	4	meV
τ_{WD}	Capture time from WL to QDash ground state	2	ps
τ_W	Recombination lifetime of WL	0.8	ns
τ_D	Recombination lifetime of QDash	0.5	ns
τ_{Spon}	Spontaneous lifetime	2.8	ns
τ_P	Photon lifetime	3.4	ps

(which is proportional to $1/\sqrt{E}$) [5]. The carrier relaxation and the re-excitation rates from WL to QDash energy states are calculated according to [5] by considering the initial relaxation time τ_{WD0} (capture time when the kth state j^{th} QDash group is unoccupied).

III. NUMERICAL RESULTS

The model is applied to calculate the lasing spectra of 1.54 μm InAs/InGaAlAs QDash laser reported in [7] at room temperature. The various parameters used in the simulation are shown in Table I, most of which are taken from [5] to model an identical QDash structure. The reason for selecting this structure stems from the fact that the laser supports only single state lasing [5] which agrees with the single-state rate equation model developed in this paper. The steady state lasing spectra are obtained by solving the rate equations simultaneously using the fourth-order Runge-Kutta numerical method up to 7.5 ns. The injected carriers are assumed to be completely available in the WL, $i.e.$ $\tau_{WS} = \tau_S = \infty$. The separation between the longitudinal optical modes is 0.354 meV, which is calculated according to [6], and the number of QDash group is 101. The inhomogeneous broadening is assumed to be Gaussian with full width at half maximum (FWHM) of 12 meV and the homogeneous broadening follows Lorentzian approximation with FWHM of 4 meV [6]. Fig. 1 shows the lasing spectra of the laser structure. Both, the experimental results (Fig. 1(a)), obtained from reference [7], and the calculated results (Fig. 1(b)), are compared. A good agreement between the simulated and the experimental results are observed. The lasing spectra at 950 mA current injection is observed at 1.545 μm and the FWHM of the lasing spectra is about 0.8 meV, including about 2 - 3 longitudinal optical modes. Moreover, a red shift in the lasing wavelength is observed on increasing the current injection (not shown due to space constraint). This may be due to band filling effect which forces the carriers to occupy higher energy states and contribute to lasing.

IV. CONCLUSION

A single-state rate equations model was presented to describe the carrier dynamics of QDash lasers. The approach has successfully modeled the spectra of the QDash laser. Currently, the model is being extended to incorporate multi-state lasing which may help to give more insights on the carrier dynamics of most of the practical QDash lasers and specifically the broadband QDash lasers which has been reported recently by Djie, et al [8].
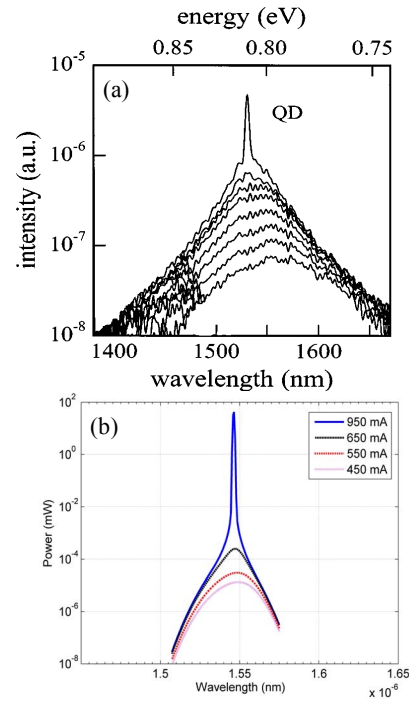

Fig. 2. (a) The electroluminescence spectra of QDash laser [7] for different injection current varying from 400 to 950 mA, and (b) the calculated lasing spectra of the QDash laser.

REFERENCES

[1] Z. Mi and P. Bhattacharya, "DC and dynamic characteristics of p-doped and tunnel injection 1.65 μm quantum dash lasers grown on InP (001)," *IEEE J. Quantum Electron. ,* vol. 42, no. 12, pp. 1224-1232, Nov 2006.

[2] M. Gioannini, "Numerical modeling of the emission characteristics of semiconductor quantum dash materials for laser and optical amplifiers," *IEEE J. Quantum Electron. ,* vol. 40, no. 4, pp. 364-373, April 2004.

[3] S. C. Heck, S. Osborne, S. B. Healy, E. P. O'Reilly, F. Lelarge, F. Poingt, O. L. Gouezigou and A. Accard, "Experimental and theoretical study of InAs/InGaAsP/InP quantum dash lasers," *IEEE J. Quantum Electron. ,* vol. 45, no. 12, pp. 1508-1515, Dec 2009.

[4] H. Dery and G. Eisenstein, "Self-consistant rate equations of self assembly quantum wire lasers," *IEEE J. Quantum Electron. ,* vol. 40, no. 10, pp. 1398-1409, Oct 2004.

[5] D. Hadass, A. Bilenca, R. Alizon, H. Dery, V. Mikhelashvili, G. Eisenstein, R. Schwertberger, A. Somers, J. P. Reithmaier, A. Forchel, M. Calligaro, S. Bansropun and M. Karkowski, "Gain and moise saturation of wide band InAs-InP quantum dash optical amplifiers: models and experiments," *IEEE J Sel. Topics in Quantum Electron. ,* vol. 11, no. 5, pp. 1015-1026, Sep/Oct 2005.

[6] M. Sugawara, K. Mukai, Y. Nakata and H. Ishikawa, "Effect of homogeneous broadning of optical gain on the lasing spectra in self-assembled InGaAs/GaAs quantum dot lasers," *Physical Rev. B. ,* vol. 61, no. 11, pp. 7595-7603, March 2000.

[7] R. Schwertberger, D. Gold, J. P. Reithmaier and A. Forchel, "Long wavelength InP based quantum dash lasers," *IEEE Photon. Technol. Lett.,* vol. 14, no. 6, pp. 735-737, June 2002.

[8] B. S. Ooi, H. S. Djie, Y. Wang, C. L. Tan, J. C.M. Hwang, X.M. Fang, J. M. Fastenau, W.K. Liu, G. T. Dang, and W. H. Chang "Quantum dashes on InP substrate for broadband emitter applications", *IEEE J. Sel. Topics Quantum Electronic.,* vol. 14, pp. 1230-1238, July/August, 2008.